

# Power Consumption Trade-Off between Power Amplifier OBO, DPD, and Clipping and Filtering

Sandrine Boumard, Mika Lasanen, Cédric Cassan, Jean-Philippe Verdeil, Jérôme David, and Ludovic Pichon  
 Olli Apilo, Atso Hekkala, Freescale Semiconductor, Inc. Thomson Broadcast - ARELIS Group  
 VTT, Oulu, Finland Toulouse, France Conflans-Sainte-Honorine, France  
 Email: name.surname@vtt.fi Email: name.surname@freescale.com Email: name.surname@arelis.com

**Abstract**—This paper investigates the trade-off between power amplifier (PA) nonlinearity, output power backoff (OBO), digital predistortion (DPD), and clipping and filtering (CF) in terms of energy consumption. The energy efficiency of a PA depends on the OBO of the signal and usually increases as the OBO decreases. Peak to average power ratio (PAPR) reduction methods like CF and PA linearization algorithms like DPD methods allow the use of a smaller OBO. Those algorithms show best results when used together. By studying the trade-off between the power consumed in the CF and DPD circuits versus having a larger OBO for a target bit-error rate (BER), we show that below a certain PA output power the power consumption is not reduced by decreasing the OBO. We also show that the increase in distortion noise when using DPD and CF might defeat the purpose of their use in terms of power consumption. Given the trend toward smaller cells like femtocells, requiring less output power, CF and DPD may not be required at all, leading to a simpler and power saving transmitter design.

## I. INTRODUCTION

Power efficiency is a very important matter in cellular telecommunications nowadays. In the past, the power amplifier (PA) has been by far the most power consuming element in a transmitter and thus its efficiency has been the key to save power. However, in smaller cells like femtocells, the power consumed in the PA is comparable to the power consumed in the other parts of the transmitter [1]. Hence, the methods used to improve the PAs efficiency and their power consumption must be revisited in order to assess their true benefits in terms of power saving. The current femtocell transmitters use linear PAs that are not energy efficient but cost-effective. With the expected denser deployment of small cells in Beyond 4G (B4G) and 5G systems [2], more energy efficient but non-linear PAs may be needed to reduce the overall energy consumption. The focus here is on the orthogonal frequency division multiple (OFDM) type of 3GPP long term evolution advanced (LTE-A) system, but the same reasoning can be applied to other transmission methods.

Semiconductor power amplifiers (PAs) are at the front end of the transmitter and amplify the signal before it is sent to the channel [3]. PAs are characterized by their gain, their linearity and their efficiency, which vary according to the input signal characteristics [4]. To study the transmitter, models of the PA need to be derived. The quality and relevance of the PA model is of high importance. An overview of various nonlinear behavioral approaches has been presented in [5]. Details can

be found in the vast literature on PA models [4], [6]–[8] and model identification [8], [9].

One of the major drawbacks of OFDM transmission is the high Peak to average power ratio (PAPR) of the transmitted signal [10]. When the power is limited, it has consequences in terms of average transmitted power hence capacity. Large PAPR also forces the use of expensive digital-to-analog converters (DACs) with a large dynamic range. Still, the main problem is with the PA that must have a large linear region, where the PA exhibits poor power efficiency. There are numerous PAPR reduction techniques for OFDM [10] and there are many factors that should be considered before a specific PAPR reduction technique is chosen. The simplest and most widely used technique of PAPR reduction is to clip the parts of the signals whose amplitude is higher than a defined threshold and then to filter the results to reduce the out-of-band radiation due to the clipping [11]. Since the filtering may cause some peak regrowth, the clipping and filtering (CF) operation is repeated to reach a desired amplitude level [10]. In terms of power consumption, there is a PAPR level for which the BER reaches a minimal value [22]. This PAPR may not necessarily be the lowest possible value of PAPR, assuming the BER increases as the PAPR decreases. In [18], some PAPR methods are evaluated in terms of the total system degradation, which are PAPR reduction, energy distribution, back-off reduction, power spectral density after the PA, and BER at the receiver.

There are several linearization techniques available to mitigate the distortion caused by the PA nonlinearity [12]–[14]. Digital predistortion (DPD) linearizers generate a nonlinear-transfer characteristic that can be thought of as the inverse of the amplifier's transfer characteristics in both magnitude and phase [15], [16]. Compared to other methods they are easier to adapt and maintain. When the signal bandwidth is small, memoryless PD is enough to compensate for the PA nonlinearities [3], but memory effects must be accounted for when the signal bandwidth is large [17]. The inversion of the PA model is not straight forward for all PA models and the predistorter can sometimes be quite complicated. The choice of the PA/DPD model is thus also influenced by the identification/learning process and its computational complexity and stability. Some DPD models are known for special cases of the Volterra PA model [6], [8].

PAPR reduction methods should be used in combination

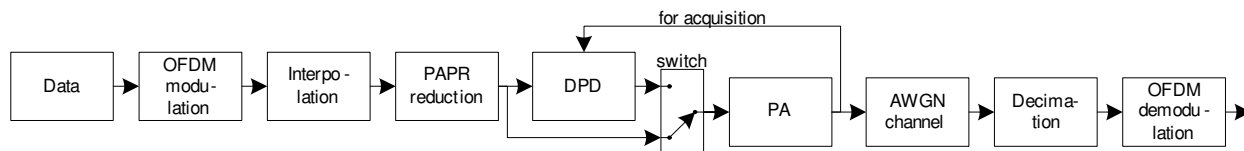


Fig. 1. Block diagram of the system.

with linearization methods [18]. The PD will mitigate the compressive gain distortion while the PAPR reduction method will reduce the clipping distortion noise [19]. The PD is more effective than the PAPR reduction method in terms of improvement in adjacent channel power ratio (ACPR), BER performance and the total degradation (TD). However, the power efficiency improvement provided by a PD is limited by the high PAPR of the signal. There are numerous examples in the literature, for example in [20], [21]. Compared to previous works, this paper provides an insight on the trade-off between using the PA in this linear behavior region, at large output power backoff (OBO), versus using it close to its saturation, at small OBO, with the help of PAPR reduction and DPD algorithms. We calculate the power efficiency and study its trade-off. In our estimations the power consumption of all the algorithms are accounted for. The rest of the paper is organized as follows. The system model is detailed in Section II. Our power consumption estimation method is then derived and described. Finally, numerical results are presented through plots to show the trends highlighted in the derivations. The conclusions are drawn in the last section.

## II. SYSTEM MODEL

The block diagram of the system is shown in Fig. 1. We focus here on a simplified 3GPP LTE-A downlink system. Random data bits are modulated to 64 quadrature amplitude modulation (64-QAM) symbols which are then transferred to the time domain through an IFFT of size  $N_{\text{FFT}}$ . A cyclic prefix is inserted and the signal is interpolated by a factor  $J$  to fit the CF sampling rate  $f_s$ . The first  $N_{\text{obs}}$  symbols are used to acquire the DPD parameters. Once the DPD has finished the acquisition phase it is used in the transmitter chain. The last part of the transmitter is the PA. For simplicity, the channel is an additive white Gaussian noise (AWGN) channel. More realistic time-varying frequency selective channel models can also be used but the main trend is expected to stay the same since the degradation induced by the PAPR reduction method and the DPD is an added noise. At the receiver side, the signal is decimated by a factor  $J$ , the cyclic prefix is removed and FFT is performed. The output bits are compared to those sent for BER evaluation. The key blocks of the system are described in more details in the following subsections.

### A. PA Modeling

The PA block is composed of a PA model modeling the nonlinearities and a soft-limiter to clip the signal. The soft-limiter is used to limit the maximum output power which cannot be modeled via the chosen PA model. A real Doherty PA

manufactured at Freescale has been measured and modeled. Several LTE signals of varying power and bandwidth have been used as test signals. Following the literature review [23], the Volterra series, pruned Volterra series, memory polynomial (MP), generalized memory polynomial (GMP) and parallel Hammerstein models have been tested. For the MP model, the output  $y(n)$  is given by

$$y_{\text{MP}}(n) = \sum_{p=1}^P \sum_{m=0}^{M-1} a_{pm} x(n-m) |x(n-m)|^{p-1}, \quad (1)$$

where  $x(n)$  is the PA input,  $P$  is the nonlinearity order,  $M$  is the memory length, and  $\{a_{pm}\}$  are the kernels' coefficients that need to be identified. The kernel refers to the simplest elements in the summation, but also the coefficient weighting it. This model can be formed into a matrix formulation that allows a simpler linear identification process. The observation time was chosen to be 200 times the number of kernels, thus varying depending on the values of  $P$ ,  $M$ , and the selected PA model. The results show that the LS identification lead to the best results and the MP and GMP models fit the Doherty PA best, both in terms of normalized mean square error (NMSE), with normalization over the estimated value, and ACPR. The MP model was chosen for the simulations.

### B. PAPR and DPD Algorithms

The CF is used as a PAPR reduction method because of its simplicity and ease of use, not requiring any additional signals nor affecting the data rate. An oversampling factor of  $J$  and  $K$  iterations are used in the algorithm. The oversampling rate affects the power consumption and must be kept as small as possible while providing adequate filtering capabilities.

The DPD algorithm will use the MP model, which is simple and widely used [17]. It is easy to identify using an indirect learning architecture and the LS algorithm. Only the acquisition phase is implemented, during which samples are used to estimate the DPD's best  $P$  and  $M$  parameters and kernels values. The number of samples during this acquisition time is 200 times the number of kernels. Those samples are not used in the BER calculations, which will be evaluated only when the DPD is in use, after the acquisition phase. The adaptation of the DPD kernel values during the transmission is not considered here.

## III. POWER CONSUMPTION STUDY

### A. Power Consumption Derivations

To compare the different approaches, both the performance and the power consumption must be investigated. The perfor-

mance will vary depending on the OBO value and the DPD and CF parameters used. The power consumption will depend on the complexity, the implementation and the characteristic of the block being investigated.

1) *Power consumption in DPD and CF blocks:* The complexity of an algorithm can be measured in terms of the Landau symbol  $O()$ , the running time of a software implementation, the numbers of parameters, or the number of operations [23]. Another important problem in behavioral model complexity is where the complexity originates from. The computational complexity can be classified into identification complexity, running complexity, and adaptation complexity [23]. The identification complexity can be left aside since it is assumed it is done once offline. The complexity of the DPD is assessed through the algorithm mathematical expression. The method presented in [23] is used to estimate the complexity. Redundancies, preconstruction, and delayed versions are all accounted for to get a more accurate complexity estimate. The computational complexity of the MP DPD is thus given in Table I. It is to be noted that in these calculations the effect of the wordlengths as well as data storage and communication are not included as they are highly dependent on the chosen hardware and architecture.

TABLE I  
COMPUTATIONAL COMPLEXITY ESTIMATE FOR THE MP DPD MODEL.

Operation	Quantity
Complex addition	$P \cdot M - 1$
Complex-real multiplication	$P - 1$
$ \cdot ^2$	1
Complex-complex multiplication	$P \cdot M$
Square-root	1

The complexity of the CF PAPR reduction method needs to be estimated as well. The filter is simply a low-pass filter to eliminate the out-of-band radiation resulting from the clipping. The filter can be implemented in the time or the frequency domain. Assuming the filter is implemented in the frequency domain and the cost of clipping is ignored, the results presented in [24] [25] can be used. Those results consider a fixed-point digital signal processor (DSP), and the energy consumption for a FFT of size  $N_{\text{FFT}}$ , power of 2, is formulated by calculating the number of cycles needed for its operation. In Table III in [24] the number of cycles for different operation is detailed. The energy consumption per cycle is also given as  $E_{\text{cycle}} = 415.8 \text{ pWsec/cycle}$ . However, this values dates from 2004. Following recent information for DSP from TI, a more accurate value is

$$E_{\text{cycle}} = 150 \frac{\text{pWs}}{\text{cycle}}. \quad (2)$$

For comparison purposes, it is assumed that both the PA and the DSP work for the same amount of time so that the computational cost can be written in W instead of J. The power consumed in the CF methods during one OFDM symbol is given by

$$P_{\text{CF}} = E_{\text{cycle}} \cdot (2K + 1) \cdot (306 + \frac{5}{2} J N_{\text{FFT}} \log_2 \frac{J N_{\text{FFT}}}{2}), \quad (3)$$

Following the same DSP implementation, the MP DPD's complexity can also be described as number of cycles per samples. The power consumed per samples for the MP DPD is given by

$$P_{\text{DPD}} = E_{\text{cycle}} \cdot (\frac{7}{2} \cdot P \cdot M + \frac{9}{2}). \quad (4)$$

2) *PA power efficiency:* The power efficiency of a PA indicates how much power is needed by the PA to amplify a signal at a certain output power. It is defined as the ratio of the output power to the consumed power. The instantaneous power efficiency of a Doherty PA depends on the input signal power in the following manner [4]

$$\eta(P_{\text{out}}) = l \eta_{\text{max}} \begin{cases} \sqrt{\gamma_{\text{OBO}}} & 0 < \gamma_{\text{OBO}} \leq \frac{1}{l^2} \\ \frac{\gamma_{\text{OBO}}}{(l+1)\sqrt{\gamma_{\text{OBO}}}-1} & \frac{1}{l^2} < \gamma_{\text{OBO}} < 1, \end{cases} \quad (5)$$

with  $\eta_{\text{max}} = \pi/4$ ,  $\alpha < 1$ ,  $l$  is a fixed positive integer that depends on the implementation,  $\gamma_{\text{OBO}} = \frac{P_{\text{out}}}{P_{\text{max}}}$  is the power loading factor and is related to the OBO via  $\text{OBO} = 10 \log_{10}(\gamma_{\text{OBO}}^{-1})$ ,  $P_{\text{out}}$  is the output power, and  $P_{\text{max}}$  is the PA's maximum output power. The value  $l = 3$  corresponds to the Doherty PAs that have been measured for this study.

Due to its nature, the OFDM signal has not a constant envelope, hence the power efficiency needs to be averaged. There are two ways to average the power efficiency [26]

$$\eta_1 = \frac{E[P_{\text{out}}]}{E[P_{\text{max}}]} \text{ and } \eta_2 = E \left[ \frac{P_{\text{out}}}{P_{\text{max}}} \right] = E[\eta(P_{\text{out}})] \quad (6)$$

These averages are not equivalent when the instantaneous efficiency depends on  $P_{\text{out}}$ .  $\eta_1$  corresponds to the definition given in [26] and is the most often used.  $\eta_2$  is the value used in [27]. Given the shape of the curve  $\eta(P_{\text{out}})$ ,  $\eta_2$  yields more pessimistic results than  $\eta_1$  and will hence be used here. Following the results in [27], assuming the OFDM signal corresponds to a Gaussian signal, the average power efficiency can be calculated via

$$\hat{\eta}_{\text{OFDM}}(P_{\text{out}}) = \int_0^{\frac{P_{\text{max}}}{P_{\text{out}}}} \eta(P_{\text{out}}|x|^2) e^{-|x|^2} d|x|^2 + \eta(P_{\text{max}}) \int_{\frac{P_{\text{max}}}{P_{\text{out}}}}^{\infty} e^{-|x|^2} d|x|^2. \quad (7)$$

Using curve fitting, the average efficiency can be modeled as

$$\hat{\eta}_{\text{OFDM}}(P_{\text{out}}) \approx c_1 + c_2 \cdot 10 \cdot \log_{10}(\gamma_{\text{OBO}}) = 76.4 - 2.5 \cdot \text{OBO}. \quad (8)$$

3) *Power consumption comparison:* The overall power consumption in the transmitter is difficult to assess, unless specific configurations are implemented and measured, which reduces the level of abstraction of the comparison. The focus is here on the CF, DPD and PA and combination of those blocks, so the power estimation will only be estimated for those blocks. The DAC, whose power consumption depends on the PAPR and the SNR, is not taken into account here either. The acquisition and adaptation of the DPD parameters will not be studied here.

The acquisition can be done offline and the adaptation might not be needed very often either. We thus obtain

$$P_{\text{Total}} = P_{\text{CF}}(N_{\text{FFT}}, J, K) + P_{\text{DPD}}(f_s, M, P) + P_{\text{PA}}(\gamma_{\text{OBO}}), \quad (9)$$

with  $P_{\text{PA}}(\gamma_{\text{OBO}}) = P_{\text{out}}/\eta(\gamma_{\text{OBO}})$ . The output power  $P_{\text{out}}$  depends on the expected performance at the receiver side. Because we have clipped the signal and because the DPD cannot correct all the nonlinearities of the PA, the needed output power to keep the BER constant at the receiver side might be larger than when we have not clipped nor predistorted the signal and used a larger OBO. We thus have two cases:

- Case A: a large OBO requires no clipping nor DPD, the transmitter is considered linear and the needed output power is  $P_{\text{out,A}}$  and the power consumed is  $P_A$ ,
- Case B: a small OBO requires clipping and DPD, this increases the distortion noise and the needed output power is  $P_{\text{out,B}} \geq P_{\text{out,A}}$  and the power consumed is  $P_B$ .

It becomes advantageous to use the CF and DPD algorithms when  $\Delta P = P_A - P_B > 0$  with

$$\Delta P = P_{\text{PA}}(\gamma_{\text{OBO,A}}) - P_{\text{Clipping}}(N_{\text{FFT}}, J, K) - P_{\text{DPD}}(f_s, M, P) - P_{\text{PA}}(\gamma_{\text{OBO,B}}). \quad (10)$$

Using (3), (4), and (8), the power difference can be expressed as

$$\begin{aligned} \Delta P &= \frac{P_{\text{out,A}}}{\hat{\eta}_{\text{OFDM}}(\gamma_{\text{OBO,A}})} - \frac{P_{\text{out,B}}}{\hat{\eta}_{\text{OFDM}}(\gamma_{\text{OBO,B}})} \\ &\quad - E_{\text{cycle}} \cdot (2K + 1) \cdot \left(306 + \frac{5}{2} J N_{\text{FFT}} \log_2 \frac{J N_{\text{FFT}}}{2}\right) \\ &\quad - E_{\text{cycle}} \cdot N_s \cdot \left(\frac{7}{2} \cdot P \cdot M + \frac{9}{2}\right) \\ &= \frac{P_{\text{out,A}}}{\hat{\eta}_{\text{OFDM}}(\gamma_{\text{OBO,A}})} - \frac{P_{\text{out,B}}}{\hat{\eta}_{\text{OFDM}}(\gamma_{\text{OBO,B}})} - C_B, \end{aligned} \quad (11)$$

where  $N_s$  is the average number of samples per OFDM symbol and  $C_B$  is the energy spent in the CF and DPD circuits, a constant not depending on the output power.

### B. Numerical Results

The expression in (11) can be looked at more precisely using the value in (2) and Matlab BER simulations. The simulation parameters are based on the 3GPP LTE system and are presented in Table II. The limit in maximum transmit rms power in picocell is usually 21 dBm, while 17 dBm is a common value in femtocells [1]. Channel SNR refers to the received SNR, at the input of the receiver.

Following the uncoded BER simulation results, it was found that, for case A,  $\gamma_{\text{OBO,A}} = 21$  dB is suitable. For case B, we have used 2 CF iterations, which helps keep the degradation minimum while keeping ACPR levels low. An example of the uncoded BER results is shown in Fig. 2 for which the DPD parameters are those which lead to the best BER results. No results are shown for the case when no DPD is used since the BER degradation is too large. The  $\Delta P$  curves are shown in Fig. 3 using the same CF, DPD and OBO parameters than in Fig. 2. The results show that below a certain output power, the power saved by using the CF and DPD combination is

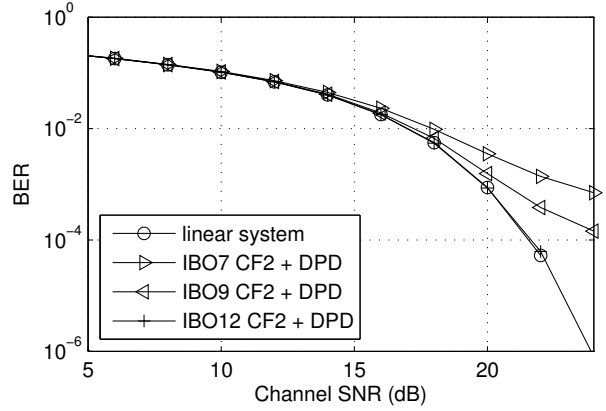


Fig. 2. BER results for the case A and case B for various OBO and number of CF iterations. OBOX refers to an OBO of X dB and CFY to Y iterations in the CF.

small, even negative below 13 dBm for an OBO of 13 dB, for example. If we were to use realistic power consumption measurements,  $\Delta P$  might even be negative at higher output power values.

Looking at Fig. 2, compared to case A, in case B with an OBO of 9 dB and CF with two iterations one more dB of power is needed in the output power for a BER target of  $10^{-3}$ . When aiming at equal BER performance, it is clear that when using the CF and DPD, the distortion noise has to be kept minimal, so that there is no need for a higher transmitted power to keep the same BER at the receiver side. In other words, when there is noise degradation, the use of CF and DPD does not lead to power savings, since a higher transmitting power is needed to reach the same BER target. The OBO must be large enough to be able to correct the PA nonlinearities via the use of CF and DPD. Below a certain OBO level, degradations occur that cannot be reversed. This OBO level not only depends on the PA but also the PAPR reduction and DPD methods used.

TABLE II  
SIMULATION PARAMETERS.

Parameters	Values
PA model	GMP
DPD model	MP, LS identification
Signal bandwidth	5 MHz
Signal modulation	64-QAM
FFT size	512
Number of used subcarriers	300
Number of symbols per slot	7
Cyclic prefix length	160 (1st symbol) 144 otherwise
$J$	6
Number of slots	100

### IV. CONCLUSION

PAPR reduction methods and DPD algorithms help lower the power consumption of transmitters by making it possible to have a smaller OBO, hence using the PA closer to its maximum power efficiency working region. However this holds when the PA is the element that consumes most of the

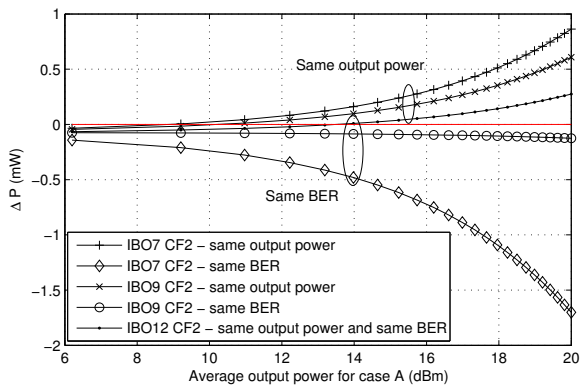


Fig. 3. Power consumption in case A minus power consumption in case B for various OBO and number of CF iterations.

power in the system. The focus is here on what happens when the output power is not very high, for example in femtocells. The PA still consumes a lot of power but the power dissipated in the other circuits must also be accounted for. The power consumption calculations only estimate the power consumed in a CF, a MP DPD and a PA, but can be easily changed to other methods and can also integrate other parts of the system. When considering the same target BER, it does not save power to use CF and DPD when the resulting degradation noise requires a larger transmitted power. The results also show that the automatic use of a PAPR reduction method and a DPD must be revisited in terms of power saving for cases when the output power is not large and the power dissipated in the circuits other than the PA cannot be ignored. This is a very important topic since an increase in the deployment of small cells is one of the keys enabling future systems to cope with traffic growth, for example.

#### ACKNOWLEDGMENT

This work was done in the framework of the Celtic-Plus OPERA-Net2 project that is partly funded by Tekes, the Finnish Funding Agency for Innovation (decision number 40446/11), and the French Ministry of Industry. The authors would like to thank their colleague Aarne Mämmelä for the numerous comments, corrections and help.

#### REFERENCES

- [1] M. A. Imran *et al.* (2010, Dec.). Energy efficiency analysis of the reference systems, areas of improvements and target breakdown. INFO-ICT-247733 EARTH D2.3. [Online]. Available: <https://www.ict-earth.eu/publications/deliverables/deliverables.html>
- [2] L. M. Correia *et al.* A Strategy for innovation in future networks in Europe. eMobility NetWorld Deliverable D1.4. 2012.
- [3] S. C. Cripps, *RF Power Amplifiers for Wireless Communications*, 2nd ed. Artech House, 2006.
- [4] J. Joung, C. K. Ho, and S. Sun, "Spectral efficiency and energy efficiency of OFDM systems: impact of power amplifiers and countermeasures," *IEEE J. Sel. Areas Commun.*, vol. 32, pp. 208–220, Feb. 2014.
- [5] J. C. Pedro and S. A. Maas, "A comparative overview of microwave and wireless power-amplifier behavioral modeling approaches," *IEEE Trans. Microw. Theory Techn.*, vol. 53, pp. 1150–1163, Apr. 2005.

- [6] M. Isaksson, D. Wisell, and D. Rnnow, "A comparative analysis of behavioral models for RF power amplifiers," *IEEE Trans. Microw. Theory Techn.*, vol. 54, pp. 348–359, Jan. 2006.
- [7] A. Zhu, J. C. Pedro, and T. R. Cunha, "Pruning the Volterra series for behavioral modeling of power amplifiers using physical knowledge," *IEEE Trans. Microw. Theory Techn.*, vol. 55, pp. 813–821, May 2007.
- [8] D. R. Morgan, Z. Ma, J. Kim, M. G. Zierdt, and J. Pastalan, "A generalized memory polynomial model for digital predistortion of RF power amplifiers," *IEEE Trans. Signal Process.*, vol. 54, pp. 3852–3860, Oct. 2006.
- [9] A. Hagenblad, "Aspects of the Identification of Wiener Models," PhD Thesis Division of Automatic Control, Department of Electrical Engineering, Linköping universitet, Sweden, 1999.
- [10] T. Jiang and Y. Wu, "An overview: Peak-to-average power ratio reduction techniques for OFDM signals," *IEEE Trans. Broadcast.*, vol. 54, pp. 257–268, June 2008.
- [11] H. Ochiai and H. Imai, "Performance analysis of deliberately clipped OFDM signals," *IEEE Trans. Commun.*, vol. 50, pp. 89–101, Jan. 2002.
- [12] A. Katz, "Linearization: reducing distortion in power amplifiers," *IEEE Microw. Mag.*, vol. 2, pp. 37–49, Dec. 2001.
- [13] P. B. Kenington, *High-Linearity RF Amplifier Design*. Norwood, MA: Artech House, 2000.
- [14] F. H. Raab, P. Asbeck, S. Cripps, P. B. Kenington, Z. B. Popovic, N. Pothecary, J. F. Sevic, and N. O. Sokal, "Power amplifiers and transmitters for RF and microwave," *IEEE Trans. Microw. Theory Techn.*, vol. 50, pp. 814–826, Mar. 2002.
- [15] J. Macdonald, "Nonlinear distortion reduction by complementary distortion," *IRE Trans. Audio*, vol. 7, pp. 128–133, Sept. 1959.
- [16] J. K. Cavers, "Amplifier linearization using a digital predistorter with fast adaptation and low memory requirements," *IEEE Trans. Veh. Technol.*, vol. 39, pp. 374–382, Nov. 1990.
- [17] L. Ding, G. T. Zhou, D. R. Morgan, Z. Ma, J. S. Kenney, J. Kim, and C. R. Giardina, "A robust digital baseband predistorter constructed using memory polynomials," *IEEE Trans. Commun.*, vol. 52, pp. 159–165, Jan. 2004.
- [18] C. Ciochina, F. Buda, and H. Sari, "An analysis of OFDM peak power reduction techniques for WiMAX systems," in *Proc. ICC*, 2006, vol. 10, pp. 4676–4681.
- [19] M. Y. Cheong, H.-L. Mttinen, S. Werner, and S.-G. Haggman, "A combined PAPR reduction and predistorter scheme for OFDM systems in nonlinear channels," in *Proc. IEEE Radio and Wireless Symp.*, 2007, pp. 309–312.
- [20] M. Helaoui, S. Boumaiza, A. Ghazel, and F. M. Ghannouchi, "Power and efficiency enhancement of 3G multicarrier amplifiers using digital signal processing with experimental validation," *IEEE Trans. Microw. Theory Techn.*, vol. 54, pp. 1396–1404, June 2006.
- [21] C. Nader, P. N. Landin, W. Van Moer, N. Bjrsell, and P. Handel, "Performance evaluation of peak-to-average power ratio reduction and digital pre-distortion for OFDM based systems," *IEEE Trans. Microw. Theory Techn.*, vol. 59, pp. 3504–3511, Dec. 2011.
- [22] D. Wulich, "Definition of efficient PAPR in OFDM," *IEEE Commun. Lett.*, vol. 9, pp. 832–834, Sept. 2005.
- [23] A. S. Tehrani, H. Cao, S. Afsardoost, T. Eriksson, M. Isaksson, and C. Fager, "A comparative analysis of the complexity/accuracy tradeoff in power amplifier behavioural models," *IEEE Trans. Microw. Theory Techn.*, vol. 58, pp. 1510–1520, June 2010.
- [24] R. J. Baxley and G. T. Zhou, "Power savings analysis of peak-to-average power ratio reduction in OFDM," *IEEE Trans. Consum. Electron.*, vol. 50, pp. 792–798, Aug. 2004.
- [25] A. K. Gurung, F. S. Al-Qahtani, A. Z. Sadik, and Z. M. Hussain, "Power savings analysis of clipping and filtering method in OFDM systems," in *Proc. ATNAC*, 2008, pp. 204–208.
- [26] H. Ochiai, "An analysis of band-limited communication systems from amplifier efficiency and distortion perspective," *IEEE Trans. Commun.*, vol. 61, pp. 1460–1472, Apr. 2013.
- [27] S. Boumard and A. Mämmelä, "The effect of power control on the average power amplifier efficiency," in *Proc. IEEE PIMRC*, 2010, pp. 629–633.